2017 International Conference on Rehabilitation Robotics (ICORR)
QEII Centre, London, UK, July 17-20, 2017.

BioMot Exoskeleton - Towards a Smart Wearable Robot for Symbiotic Human-Robot Interaction

Tomislav Bacek[1], Marta Moltedo[1], Kevin Langlois[1], Guillermo Asin Prieto,[2], Maria Carmen Sanchez-Villamañan[2], Jose Gonzalez-Vargas[2], Bram Vanderborght[1], Dirk Lefeber[1] and Juan C. Moreno[2]

***Abstract*— This paper presents design of a novel modular lower-limb gait exoskeleton built within the FP7 BioMot project. Exoskeleton employs a variable stiffness actuator in all 6 joints, a directional-flexibility structure and a novel physical human-robot interfacing, which allows it to deliver the required output while minimally constraining user's gait by providing passive degrees of freedom. Due to modularity, the exoskeleton can be used as a full lower-limb orthosis, a single-joint orthosis in any of the three joints, and a two-joint orthosis in a combination of any of the two joints. By employing a simple torque control strategy, the exoskeleton can be used to deliver user-specific assistance, both in gait rehabilitation and in assisting people suffering musculoskeletal impairments. The result of the presented BioMot efforts is a low-footprint exoskeleton with powerful compliant actuators, simple, yet effective torque controller and easily adjustable flexible structure.**

I. INTRODUCTION

Human daily activities, including locomotion, are a product of the complex interplay between neural and musculoskeletal systems. An outcome of this interplay is the flexibility of real-time human adaptability when confronted with both task and environmental constraints. Despite their indisputable benefit, wearable robots (WRs) are still presenting constraints for human wearers due to a lack of a proper physical human-robot interface (pHRI) and robot's versatility, coming mainly from the actuation system.

The main goal of the BioMot project [1] was to explore and exploit dynamic sensory-motor interplays in order to achieve seamless interaction and safe locomotion adjusted to the user's intentions and capabilities. A hallmark in the process of moving WRs into a constrained daily life environment are smart, compliant actuation units which, when accompanied by a proper pHRI, have the potential to assist the human body in achieving desired dynamic motions.

Compliance, although important in human locomotion [2], is yet to find its way to commercial WRs. Currently available commercial WRs, such as ReWalk™ 6.0 [3], REX [4], Ekso GT [5], Indego® [6] and HAL5® [7], all use direct-drive actuators, and so does the commercially available gait therapy device Lokomat [8]. A different situation can be seen in the research prototypes where devices such as LOPES [9], IHMC [10] and MINDWALKER [11] are pointing towards a new trend of bringing compliant actuators into WRs to exploit their advantages over the traditional stiff actuation. Yet another step forward are devices that use Variable Stiffness Actuators (VSAs) [12] which allow embodiment of characteristics found in biological systems in the new generation mechatronic systems. Devices that employ variable stiffness include ALTACRO stationary gait WR [13], and MIRAD [14] and ATLAS [15] exoskeletons.

However, compliance itself is not sufficient to ensure safe actuation and it should be complemented by the appropriate control strategies [16]. As discussed in [17] and [18], controllers that have been used in the literature vary substantially depending on the application and functionality of the actuation unit. Moreover, the exact control algorithms of many exoskeletons are not well documented, especially for commercial systems.

Fig. 1. BioMot gait exoskeleton. All the joints are actuated using the spindle-driven MACCEPA, a VSA, active only in the sagittal plane (knee joint actuator employs also spring in parallel to exploit spring-like behavior of the biological joint). In addition to these 6 active DoFs, 4 passive DoFs are available due to exoskeleton's directional flexibility, which imposes minimal constraints onto the gait. The entire exoskeleton structure - hip module, frame and foot plates, is designed within the project, guided by user comfort, short donning time, low footprint and structural stability. The weight of the exoskeleton, including electronics, backpack with the CPU, and the batteries, is 19.4 kg (the batteries themselves have 3.1 kg, since design of a lightweight and efficient portable power supply was not one of the project goals).

*The presented work was developed within the project BioMot (European Commission's 7th Framework Program, Grant Agreement number IFP7-ICT-2013-10-611695) and it is supported by FWO project (no.G026214N).

[1]T. Bacek, M. Moltedo, K. Langlois, B. Vanderborght and D. Lefeber are with the Department of Mechanical Engineering, Robotics & Multibody Mechanics Research Group, Vrije Universiteit Brussel, 1050 Brussel, Belgium and with Flanders Make, tomislav.bacek@vub.ac.be

[2]G. Asin Prieto, M.C. Sanchez-Villamañan. J. Gonzalez-Vargas and J.C. Moreno are with the Bioengineering Group, Consejo Superior de Investigaciones Cientficas (CSIC), 28500 Madrid, Spain

Nevertheless, some trends can be identified. In [19], seven different control strategies are identified, dominated by a predefined gait trajectory control (used in ReWalk™, Ekso, HAL®, IHMC, MINDWALKER, Indego). Joint position control is also identified as the main control approach in [17], along with the force/torque control. This strategy is useful when the user has little ability to interact with or control the exoskeleton. Force control, on the other side, allows the implementation of the so-called assist-as-needed (AAN) paradigm [20] by applying corrective force fields adaptable to specific patient's needs, thus allowing human error and adaptation. This paradigm recently took a swing and has been used in MIRAD and Ekso exoskeletons and Lokomat.

Another important aspect in the overall exoskeleton design is pHRI, since all the loads coming from the actuator are transmitted via pHRI to the user's limbs, thereby affecting the overall performance of the exoskeleton. As noted in [17], pHRI and user comfort are still an issue and much research is yet to be carried out in order to define the quantifiable parameters of a pHRI design that will result in a safe, comfortable and efficient transfer of the loads. Some valuable efforts towards this can be found in studies which attempt to define kinematic design parameters for pHRI [21].

Within the BioMot project, a successful contribution has been made in all three aspects of the overall exoskeleton design. All the joints of the BioMot exoskeleton (Fig. 1) are actuated by the novel spindle-driven joint-specific MACCEPA VSA [22] due to its simplicity, compactness, robustness and favourable output characteristic. The knee joint actuator, in addition to MACCEPA, also employs spring in parallel to exploit spring-like behavior of the biological joint. Although initially controlled in a zero-torque and a feed-forward mode, a simple position-based control approach is being implemented that makes the actuator a torque source as seen from the joint. This way it is going to be possible to implement the user-specific AAN control strategy. In the end, this smart actuator is accompanied by a lightweight, low-footprint and ergonomic pHRI developed within the BioMot project, the result of which is depicted in Fig. 1.

The remainder of this paper is organized as follows. Section II gives an overview of the developed compliant technology and its (quasi-static) performance. Section III describes control strategies applied to the BioMot exoskeleton, while Section IV presents newly developed pHRI and exoskeleton structure. Section V gives concluding remarks.

II. COMPLIANT ACTUATION TECHNOLOGY

Within the BioMot project, two generations of VSA have been developed for use in exoskeletons and/or joint orthoses, based on the same (MACCEPA) concept. Nevertheless, the two generations differ significantly in their realizations, with the second one being a multidimensional upgrade of the first one. The second generation is presented in the sequel.

A. Conceptual design of the actuators

MACCEPA [22] is a torque-controlled VSA working as a torsion spring that allows independent control of equilibrium position and joint stiffness. Different realizations of the MACCEPA concept have been successfully applied in the bipedal walkers [23], prosthesis [24], stationary gait rehabilitation robot [13] and a mobile sit-to-stance exoskeleton [14]. To improve the performance of these actuators, and similar to the ankle orthosis [25], BioMot exoskeleton uses a highly efficient spindle-driven MACCEPA, leading to better actuator inertia distribution and a more compact design.

The conceptual design of all the BioMot exoskeleton joint actuators is the same (see [25], [26] for more details), but due to different kinematic/kinetic requirements, their realization is different. For example, a spring acting in parallel (PS) to the knee joint is employed in order to exploit changes in gravitational potential energy during gait. The shape of all the actuators is guided by an anthropomorphic design approach, leading to revolute joint-actuators providing a torque in the sagittal plane. All the actuators are designed with the goal of providing the same peak torque of minimally 50Nm. This value comes from a capability gap analysis conducted within the BioMot project (the capability gap is the difference between the torque provided by a healthy and impaired subject). Actuator design parameters and drive-train components were all obtained from a simulation study performed in Matlab®, where energy requirements of the actuators to deliver both natural [27] and incomplete spinal chord injury (iSCI) patients' walking patterns were minimized.

The MACCEPA can change spring pre-compression online by using additional motor. However, only the equilibrium position motor is implemented in the BioMot actuators due to a wearability requirement. The pre-compression can be changed manually by means of a simple mechanism that proved to be robust and stable across different conditions. This, together with the spring being inside the lever arm, allowed the actuators to be made smaller and more compact, leading to an improved wearability and human-robot synergy. Further decrease in weight is obtained by performing a Finite Element Method (FEM) analysis to remove unnecessary material while preserving the actuators' structural integrity.

B. Actuator implementation

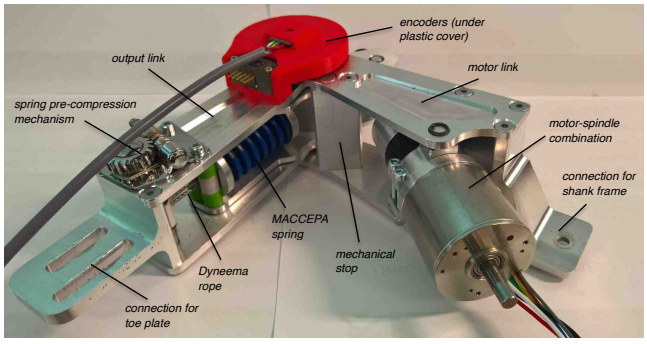

Fig. 2. Realization of the spindle-driven MACCEPA for the ankle joint. The lever arm ROM, if attached to a human as intended, is 32° in plantarflexion and 21° in dorsiflexion. The weight of the actuator is 1.18kg.

All three actuators consist of two distinctive parts - the motor side and the output side. The motor side houses a

motor-spindle combination (and a PS mechanism in the case of the knee joint), while the output side houses a lever arm, MACCEPA spring and spring pre-compression system. All three actuators share the main design attributes - spring inside the lever arm, worm-gear pre-compression mechanism with Dyneema® rope and FEM-based weight reduced structure. Two encoders are used per actuator - incremental optical and absolute magnetic for measuring the biological angle (angle between two leg segments) and spring deflection angle (angle between the actuators' lever arm and output link), respectively. The actuators' range of motion (ROM), limited by mechanical stops, and peak torque outputs, are able to provide kinematically unobstructed fully-assisted gait at the hip and the knee joints and partially assisted at the ankle, as well as partially assisted stair climbing and chair sitting. Fig. 2 depicts the ankle actuator realization.

A distinctive feature of the knee actuator (Fig. 3) is that it comprises of two springs - in series and in parallel. Namely, during gait, kinematics and kinetics of a knee joint are such that two clearly different gait phases can be observed: stiff early stance (weight-acceptance, WA) phase and compliant swing phase [26]. In order to mimic this behaviour more accurately and efficiently, a spring is added as part of a quasi-passive mechanism in parallel to the knee joint and its existing MACCEPA in-series unit.

Since this spring needs to be engaged only during the weight acceptance phase of the gait cycle, a simple EC motor-based on/off mechanism is used to (dis)engage the spring when needed. During the loading phase (WA knee flexion/extension), the spring is friction-locked in place due to a non-backdrivable spindle, thereby requiring no additional energy from the EC motor. When the loading phase ends, prior to the late stance and swing, the EC motor moves the spring so that the swing phase of the gait can take place.

Fig. 4 depicts the hip actuator realization. The design of the hip actuator was guided by two hip joint-specific requirements - very high ROM needed to perform the activities of daily life (ADLs), and a need to decrease the possibility of collision between the actuator and the upper body of the wearer (in particular wearer's arms).

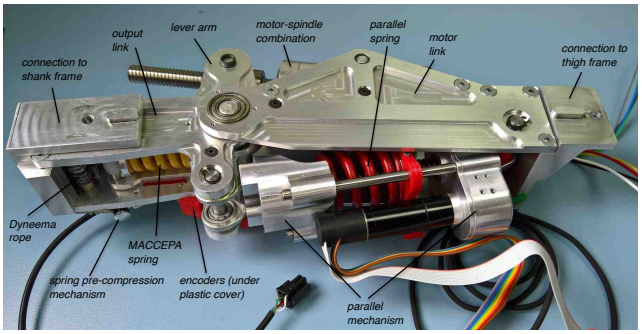

Fig. 3. Realization of the spindle-driven MACCEPA for the knee joint. The lever arm ROM is 2° in extension and 90° in flexion. The hyper-extension angle can be decreased if necessary. PS mechanism, consisting of a small motor and a spindle-guided spring, is also depicted. This mechanism reduces actuator energy consumption, while not compromising its versatility and flexibility. The weight of the actuator is 1.57kg.

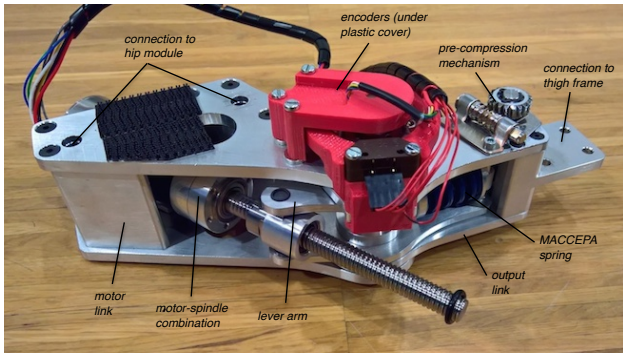

Fig. 4. Realization of the spindle-driven MACCEPA for the hip joint. The lever arm ROM, if attached to a human as intended, is 25° in extension and 102° in flexion. The weight of the actuator is 1.3kg.

C. Actuator performance

The actuators' characterization is out of the scope of this paper, so no extensive benchmarking results will be given herein. However, two important test results are shown in order to validate the performance of the actuators. Fig. 5 shows the response of the ankle actuator in the task of following biological torque trajectory, as given in [27], with peak plantarflexion torque of 50 Nm and step duration 2 seconds. The actuator can deliver this reference, despite the discrepancy seen at low torques and a shortly missed peak torque of 50 Nm. The error, together with a small phase delay, is due to the chosen gains of a PID controller.

Fig. 6 gives an overview of the simulated and experimentally obtained torque-deflection angle trajectories of the knee actuator for different MACCEPA spring pre-compression settings. Experimental trajectories exhibit hysteresis, as expected. MACCEPA's output is fairly linear (and symmetric) for all the pre-compression settings, which does deviate from the MACCEPA model at low pre-compressions [22], but is highly favourable from a control point of view. The higher the spring pre-compression, the better the model approximates the actual actuator's output.

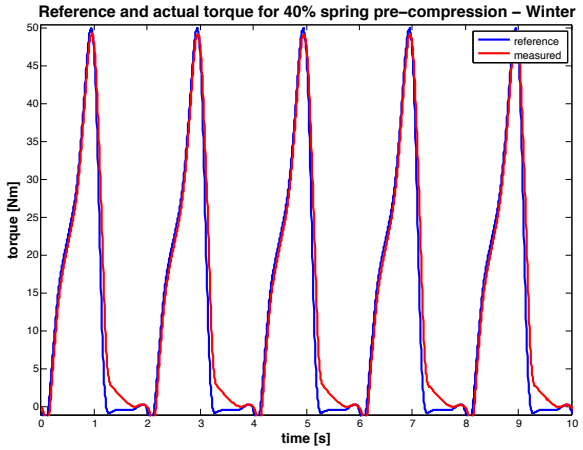

Fig. 5. The reference and the actual torque for 40% spring pre-compression setting, in the case of Winter's ankle torque trajectory data (peak torque 50 Nm and step duration 2 s). Discrepancies seen at low and peak torque, as well as a small phase delay, come from the gains of a PID controller.

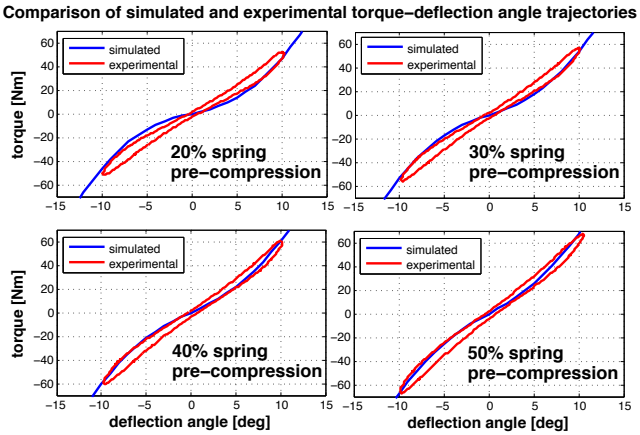

Fig. 6. An overview of the simulated and experimentally obtained torque-deflection angle trajectories of the knee actuator for different pre-compression settings. MACCEPA exhibits fairly linear and symmetric output for all the pre-compression settings, which is favourable from the control point of view. At higher pre-compressions, where the actuator is designed to work, MACCEPA model is a good approximation of the actual output.

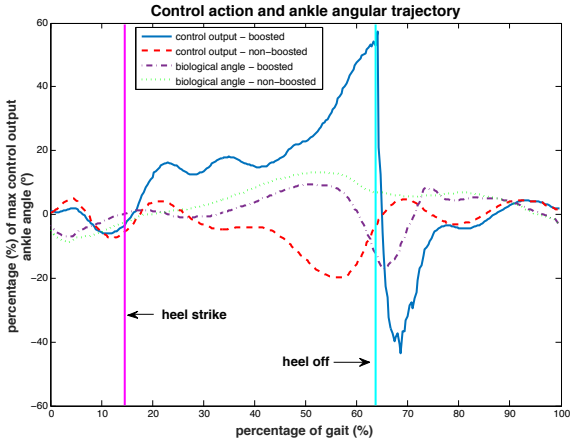

Fig. 7. Comparison of an ankle actuator control output in two steps: red dashed line and blue solid line depict control output of a non-boosted and boosted step, respectively. Vertical lines depict heel strike and heel off, which represent the beginning and the end of the control output ramp profile, respectively. Biological ankle angle in both steps is also depicted, showing increased plantarflexion angle due to the action of a boost controller.

III. Control Strategy

Currently, two control strategies have been applied to the BioMot actuators - a zero-torque mode (in all the actuators), and a feedforward energy injection during push-off (in ankle actuator only). However, MACCEPA's design allows it to be position-controlled prior to a compliant element, while acting as a torque source from the viewpoint of the joint [13]. This torque-based control approach will be applied in the upcoming tests and validation of the exoskeleton.

A. Implemented low-level control strategies

Zero-torque mode is a low-level control approach in which the actuator tries to minimize resistive torque which the user feels by driving the exoskeleton. In the case of the MACCEPA, the PID controller works by minimizing the deflection angle, since MACCEPA's torque can be directly inferred from this angle. This is a straightforward approach since the deflection angle is measured by one of the encoders.

Apart from a zero-torque mode, another low-level control strategy applied within the BioMot project is a feedforward energy injection to the ankle orthosis during push-off, in the form of a ramp boost. When the heel strike is detected using foot-switches attached to the exoskeleton's foot plates, the boost controller is activated, outputting a torque ramp profile. From that point on, until the heel-off is detected, the constantly active zero-torque controller is superimposed by the boost controller. Once the heel-off is detected, the boost controller is deactivated, and only the zero-torque mode remains active throughout the remainder of the gait cycle.

Torque amplitude of the boost reached at the heel-off can be adapted by changing the slope of the ramp. Fig. 7 shows comparison of two control actions and their effect on the ankle joint kinematics, one with inactive boost controller, and the other one where a ramp reaching almost 60% of the maximum actuator torque is applied. Boosted step clearly increased ankle plantarflexion angle, indicating assistance provided to the ankle joint during the push-off.

B. Low-level torque control strategy

From the joint point of view, the MACCEPA acts as a torsion spring. According to Hooke's law, the torsion spring torque depends on a torsional stiffness and deflection angle. A property of the MACCEPA is that its torque-angle characteristic corresponds to a torsion spring characteristic. In other words, MACCEPA's deflection angle corresponds to a torsion spring deflection angle, while the slope of its characteristic corresponds to a torsion spring stiffness.

By exploiting this property, a control approach is derived in which MACCEPA's lever arm is position controlled prior to compliant element, while the actuator acts as a torque source from the viewpoint of the joint. Details of this control approach can be found in [13]. In short, by using the information from MACCEPA encoders in real time, and pre-recording the information on the relation between MACCEPA's spring pre-compression P and torsion spring stiffness K_{ts}, i.e. by obtaining $K_{ts} = K_{ts}(P)$, it is possible to turn MACCEPA into a torque source, without having a torque sensor in the system, all while employing a simple position control. This control approach is currently being implemented in the BioMot exoskeleton.

C. Electronics

The BioMot exoskeleton is controlled by means of a distributed control architecture, depicted in Fig. 8, which allows local control loop implementations. A custom designed and developed dsPIC-based driver board (Secondary Processing Unit, SPU), applied in each exoskeleton joint, is responsible for the control of the actuated joint and sensor data acquisition, sending control output every 3 ms. The data from SPUs are then gathered and packed by a custom designed ARM-based board that is responsible for management of the CAN-bus communication towards the BeagleBone Black (BBB), a CPU, at 100 ms intervals. Interface with the BBB is implemented in Robot Operating System (ROS).

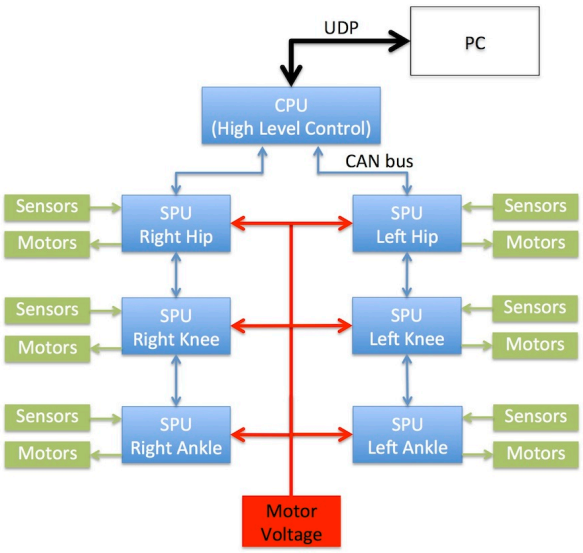

Fig. 8. A general overview of the distributed hardware architecture used with the BioMot exoskeleton. CPU (BeagleBone Black) communicates via a CAN-bus with each joint, where the local control loop is ran by an SPU.

IV. EXOSKELETON OUTLOOK

pHRI is, together with the actuation technology and control strategy, a hallmark in the design of the exoskeletons. If designed incorrectly, pHRI can significantly decrease both efficiency and effectiveness of the actuation unit. The importance of this aspect of exoskeletons is often underestimated. In the sequel, the results of the efforts within the BioMot project put into designing pHRI are presented.

A. Frame and cuffs

The goal of designing a new exoskeleton structure for the BioMot exoskeleton was to build a lightweight, comfortable and easily adjustable low-profile structure. To do so, the frame is built using spring-steel plates whose profile is chosen so as to be stiff in the sagittal plane, and flexible in other two planes, thus minimizing constraints the frame puts onto the human wearer. For practical and the frame's structural integrity reasons, two sets of plates, different in length, were designed per leg segment, resulting in a total leg segment adjustability in between 0.35 and 0.45 m. The frame's height adjustability and the steel plates' replacement are simplified by using a minimal set of easily reachable same-size screws. Each plate is fixed to the respective actuator at one end, while having a groove towards the other end to allow adjustability. Fig. 9 shows frame-cuffs setup of one leg segment.

As seen in Fig. 9, two cuffs are used per leg segment, one being at the back and another one at the front part of the segment. This way, the biggest torques exerted on the human wearer are transmitted by pushing, rather than by pulling on the cuff. The half-moon shape of the cuffs and a 3D printed flexible structure makes them easily adjustable to the user's leg shape. In order to fix the cuffs to the user's legs, an easy-to-use BOA closure system is employed. Another level of the cuffs' adjustability comes from the L-shaped spring-steel plates used to connect the cuffs to the frame, since these plates can be adjusted in both sagittal and frontal planes.

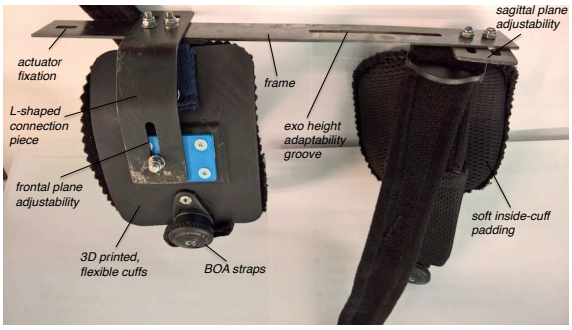

Fig. 9. The frame plate and cuffs of one leg segment. Each leg segment has two cuffs placed at the opposite side of the segment in the sagittal plane to decrease the torque transmission losses and increase comfort. Cuffs are flexible and their position is adjustable in both sagittal and frontal planes. The frame's directional flexibility allows more natural gait pattern by providing passive DoF's in addition to the active ones. Passive DoFs allow limited deflection, yet sufficient to allow more natural gait.

B. Foot-plates

The BioMot exoskeleton footplate has several distinctive features in order to allow a natural and stable walking pattern, while being able to transmit the required torques and adjust to the different users. To prevent the flat foot-drop after the heel strike, the footplate is divided into the toe and the heel plate. Both plates are slightly bent up at one end, in order to follow natural foot roll (see Fig. 10), and are built in 2 mm thick spring steel with a thin rubber underneath, which makes them slim and comfortable, yet durable enough to transmit the required torques. Furthermore, due to the adaptability of both plates in both axes of the sagittal plane (see [25]), people of different foot sizes can wear the exoskeleton, provided they fit the wearer's height constraints. Finally, the adjustability of the foot plates is made simple by using a minimal number of easily reachable same-size screws, and a combination of easy-to-use Velcro and BOA straps.

Fig. 10. Realization of the foot plates of the BioMot exoskeleton. The plates have a low footprint and are easily adjustable to different users. Two BOA straps are used at the heel plate, and a single Velcro strap at the toe plate. Both plates are slightly bent up on one side - toe plate at the toe side, heel plate at the heel side, to allow a more natural walking pattern. Intermediary links and carriage screws are used to fix the plates to a desired position with respect to the ankle actuator (and thus ankle joint axis).

C. Hip module

The hip module (Fig. 11) is made of a 3-plate aluminium structure and a commercial flexible back-spanning plate

attached to a user's trunk by the adjustable fabric belts. The aluminium structure plates include the two lateral plates that connect hip actuators to the hip module, and a back plate, which connects lateral plates forming the U-shape stiff frame. This U-shape frame is connected to the commercial back-spanning plate via an aluminium back plate. The two lateral plates can slide into the back plate, allowing the adjustment of the hip module width depending on the size of the user. The plates also have slots to allow better alignment of the hip joint and hip actuator axis in the sagittal plane. Anthropomorphic dimensions were taken into account when designing the hip module and defining the adaptability range in order to improve the user's comfort.

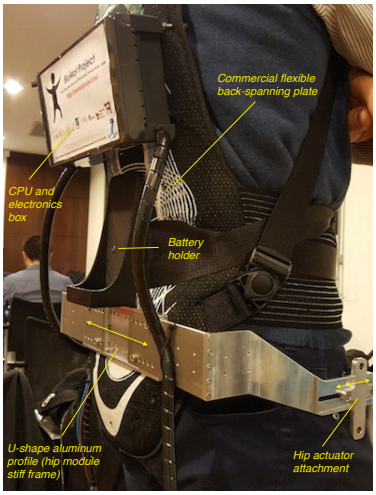

Fig. 11. Realization of the BioMot exoskeleton hip module. Three aluminium plates form a U-shape stiff frame, that is worn around the user's waist. Hip actuators are attached to the lateral sides of the frame, which is in turn connected to the commercial back-spanning plate. This plate is attached to the user trunk by adjustable fabric belts. A box containing main CPU is also attached to this plate, and so are the batteries, making the exoskeleton fully portable.

V. CONCLUSIONS

Although a lot of advancements have been taking place recently in all spheres of WRs, there is still a lot of research that needs to be done in order to fully bring these devices into the daily life of impaired people. With herein presented exoskeleton, the BioMot project gives its contribution to all three main aspects of the WR's design.

Novel, joint-specific spindle-driven VSAs have been developed, which are lightweight, robust, easy-to-control and have a high torque-to-weight ratio. In the knee joint, VSA is combined with the energy efficient spring-in-parallel mechanism in order to utilize spring-like behavior of the biological joint during gait. The presented torque control, which is currently being implemented, will allow a simple position control of the actuators, while having them acting as a torque source without a torque sensor in the system. These actuators and control strategy, when combined with a directionally-flexible, easily adjustable and lightweight pHRI developed within the project, lead to a novel modular exoskeleton of a low structural profile, powerful and robust actuation and a user-specific therapy and assistance delivery.

Future work will include conducting more tests in a zero-torque and assistive modes, in order to evaluate the overall performance of the exoskeleton. Also, the torque controller will be further developed and implemented, first in the ankle joint, and then the entire exoskeleton.

REFERENCES

[1] J.C. Moreno et al., Symbiotic wearable robotic exoskeletons: the concept of the biomot project, in: Inter. Workshop Symb. Inter., pp. 72-83, Springer International Publishing, 2014.
[2] R. Alexander, Three uses of springs in legged locomotion. International Journal of Robotics Research, Vol. 9, no. 2, pp. 53-61, 1990.
[3] ReWalk Robotics. http://www.rewalk.com, 2016
[4] REX Bionics. http://www.rexbionics.com, 2016.
[5] Ekso Bionics. http://www.eksobionics.com, 2016.
[6] Parker Hannifin Corp. http://www.indego.com, 2016.
[7] Cyberdine Inc. http://www.cyberdine.jp/english, 2016.
[8] Hocoma. http://www.hocoma.com, 2016.
[9] J.F. Veneman et al., Design of a Series Elastic- and Bowdencable-based actuation system for use as torque-actuator in exoskeleton-type training, in Proc. IEEE Inter. Conf. Rehab. Rob., pp. 496-499, 2005.
[10] H. K. Kwa et al., Development of the IHMC mobility assist exoskeleton, in IEEE Inter. Conf. Robot. Autom., pp. 2556-2562, 2009.
[11] L. Wang, S. Wang, E. H. van Asseldonk and H. van der Kooij, Actively controlled lateral gait assistance in a lower limb exoskeleton, in IEEE Int. Conf. Intell. Rob., pp. 965-970, 2013.
[12] B. Vanderborght et al., Variable impedance actuators: a review, Robotics and Auton. Systems, Vol. 61, no. 12, pp. 1601-1614, 2013.
[13] V. Grosu et al., Design of smart modular variable stiffness actuators for robotic assistive devices, submitted to Trans. Mech., 2016.
[14] K. Junius et al., Mechatronic design of a sit-to-stance exoskeleton. 5th IEEE Inter. Conf. Biomed. Rob. Biomech., pp. 945-950, 2014.
[15] M. Cestari, D. Sanz-Merodio, J.C. Arevalo and E. Garcia, An Adjustable Compliant Joint for Lower-Limb Exoskeletons, IEEE/ASME Trans. Mech., Vol. 20, no. 2, pp. 889-898, 2015.
[16] P. Beyl et al., Safe and Compliant Guidance by a Powered Knee Exoskeleton for Robot-Assisted Rehabilitation of Gait, Adv. Robotics, Special Issue, Vol. 25, no. 5, pp. 513-535, 2011.
[17] A. Young and D. Ferris, State-of-the-art and Future Directions for Robotic Lower Limb Exoskeletons, IEEE Trans. Neural. Syst. Rehabil. Eng., pp. 1-13, 2016.
[18] M.R. Tucker et al., Control strategies for active lower extremity prosthetics and orthotics: a review, Journal NeuroEng. Rehab., Vol. 12, pp. 1-29, 2015.
[19] T. Yan et al., Review of Assistive Strategies in Powered Lower-Limb Orthoses and Exoskeletons, Rob. Auton. Sys., Vol. 64, pp. 120-136, 2015.
[20] S. Srivastava et al., Assist-as-Needed Robot-Aided Gait Training Improves Walking Function in Individuals Following Stroke, IEEE Trans. Neural Syst. Rehabil. Eng., Vol. 23(6), pp. 956-963, 2015.
[21] A. Schiele and F.C.T. van der Helm, Kinematic Design to Improve Ergonomics in Human Machine Interaction, IEEE Trans. Neural Sys. Rehab. Eng, Vol. 14, no. 4, pp. 456-469, 2006.
[22] R. Van Ham et al., MACCEPA, the mechanically adjustable compliance and controllable equilibrium position actuator: Design and implementation in a biped robot, Rob. Auton. Sys., Vol. 55, no. 10, pp. 761-768, 2007.
[23] Y. Huang et al., Step length and velocity control of a dynamic bipedal walking robot with adaptable compliant joints, IEEE/ASME Trans. Mech., Vol. 18, no. 2, pp. 598-611, 2013.
[24] L.Flynn et al., Ankle-knee prosthesis with active ankle and energy transfer: Development of the CYBERLEGs Alpha-Prosthesis, Rob. Auton. Sys., Vol. 73, pp. 4-15, 2015.
[25] M. Moltedo et al., Mechanical Design of a Lightweight Compliant and Adaptable Active Ankle Foot Orthosis, IEEE Inter. Conf. Biomed. Rob. Biomech., pp. 1224-1229, 2016.
[26] T. Bacek et al., Conceptual design of a novel variable stiffness actuator for use in lower limb exoskeletons. IEEE Inter. Conf. Rehab. Rob., pp. 583-588, 2015.
[27] D. A. Winter, The biomechanics and motor control of human gait: Normal, elderly and pathological, Waterloo Biomech., Vol. 2, 1991.